Preprint Title	Synthesis of Tetracyclic Skeleton of Aspidosperma Alkaloids via PET-Initiated Cationic Radical-Derived Interrupted [2+2]/Retro-Mannich Reaction
Authors	Ru-Dong Liu, Jian-Yu Long, Zhi-Lin Song, Zhen Yang and Zhong-Chao Zhang
Publication Date	08 Aug. 2025
Article Type	Full Research Paper
Supporting Information File 1	Supporting Information-20250808.docx; 15.1 MB
ORCID® iDs	Zhi-Lin Song - https://orcid.org/0009-0009-7524-4898; Zhen Yang - https://orcid.org/0000-0001-8036-934X; Zhong-Chao Zhang - https://orcid.org/0000-0001-5017-5691

Synthesis of Tetracyclic Skeleton of Aspidosperma Alkaloids via PET-Initiated Cationic Radical-Derived Interrupted [2+2]/Retro-Mannich Reaction

Ru-Dong Liu‡[1], Jian-Yu Long‡[1], Zhi-Ling Song[1], Zhen Yang*[1,2,3] and Zhong-Chao Zhang*[1,4]

Address: [1]Laboratory of Chemical Genomics, School of Chemical Biology and Biotechnology, Peking University Shenzhen Graduate School, Shenzhen 518055, China, [2] Key Laboratory of Bioorganic Chemistry and Molecular Engineering of Ministry of Education and Beijing National Laboratory for Molecular Science, and Peking-Tsinghua Centre for Life Sciences, Peking University, Beijing 100871, China, [3] Shenzhen Bay Laboratory, Shenzhen 518055, China, [4] Key Laboratory of Structure-Based Drug Design & Discovery of Ministry of Education,Shenyang Pharmaceutical University, Liaoning Shenyang 110016, China

Email: Zhong-Chao Zhang* zc_zhang@pku.edu.cn;

Zhen Yang* zyang@pku.edu.cn

* Corresponding author

‡ Equal contributors

Abstract

Natural products with topologically complex architectures are important sources in drug discovery. The pursuit of conciseness and efficiency in the total synthesis of natural products promotes continuous innovation and the development of new reactions and strategies. In this work, a PET-initiated cationic radical-derived interrupted [2+2]/retro-Mannich reaction of N-substituted cyclobutenone provided a facile approach to the direct construction of the ABCE tetracyclic framework of Aspidosperma alkaloids. DFT calculations showed that the rate-determining step of the key PET reaction involved C19–C12 bond formation and C19–C3 bond cleavage. Investigation of the bond length changes along the IRC path, spin density, and NBO analysis indicated that this process is neither strictly concerted nor stepwise, but falls in between, and involves a formal 1,3-C shift.

Keywords

Aspidosperma Alkaloids, photoinduced electron transfer, [2+2]-Cycloaddition/*retro*-Mannich Reaction, DFT study.

Introduction

Photochemical reactions, which enable the construction of topologically complex architectures from simple building blocks, have attracted considerable attention in recent decades. Numerous approaches to natural product synthesis have been reported in which a photochemical transformation represents a key step[1,2,3]. In this context, photochemical [2+2] cycloaddition and subsequent fragmentation of the resulting cyclobutane provides a valuable strategy for synthesizing natural and unnatural products from simple building blocks [4]. Three distinct photoinitiated approaches have been established for the formation of [2+2] cycloadducts: direct irradiation[5,6], energy transfer (EnT) [7] and photoinduced electron transfer (PET, or photoredox catalysis) processes[8,9,10].

Cyclobutenone (**A**) is a versatile C4 synthon[11]; its [2+2] photocyclization yields **B**, featuring a strained bicyclo[2.2.0]hexane unit[12], which can fragment to form **C** (Figure 1a) [13,14]. However, competitive C1–C4 bond cleavage under irradiation or heating leads to ketene **D**, which isomerizes to **E**. This fragmentation pathway dominates under various conditions (e.g., transition-metal catalysis, nucleophilic addition), driven by ring-strain release[11].

PET, an alternative to direct excitation and EnT, enables unique radical intermediates[9,10]. We previously demonstrated the Ir-catalysed [2+2] cyclization/retro-Mannich reaction of a tryptamine-substituted cyclopentenone **F**, which led to the formation of indoline **J** (Figure 1b)[15]. Unlike other reported methods[16,17,18] the PET reaction of **F** generates the cationic radical **G**, which initiates formation of **H**, which has a strained bicyclo[3.2.0]heptane core. Strain release of **H** triggers a downstream radical-driven retro-Mannich reaction, which ultimately results in the formation of **J** via reductive quenching of intermediate **I**.

As part of our current interest in the synthesis of complex natural products via photochemical reactions, we decided to achieve such an unusual bond cleavage (Figure 1a, path A) of cyclobutenone by generating a radical cation species via a PET

reaction. The synthetic plan is shown in Figure 1c; PET-initiated [2+2] cyclization of the tryptamine-substituted cyclobutenone **K** enables the formation of the radical cation **L**, which has a highly functionalized and rigid bicyclo[2.2.0]hexane core. Fragmentation of the C3–C19 bond affords a redox active intermediate and further reductive quenching affords the tetracyclic indoline **M**, which was expected to serve as a common intermediate for the total synthesis of *Aspidosperma* alkaloids. These alkaloids constitute a large family of structurally complex compounds, which incorporate a pentacyclic ABCDE skeleton (Figure 1d, **1**–**8**)[19,20,21,22,23]. However, the formation of intermediate **L** is challenging because its ring-strain energy (Figure 1e, 52.1 kcal/mol) is higher than that of its counterpart, i.e. the bicyclo[3.2.0]heptane motif (28.3 kcal/mol) in **H**[24].

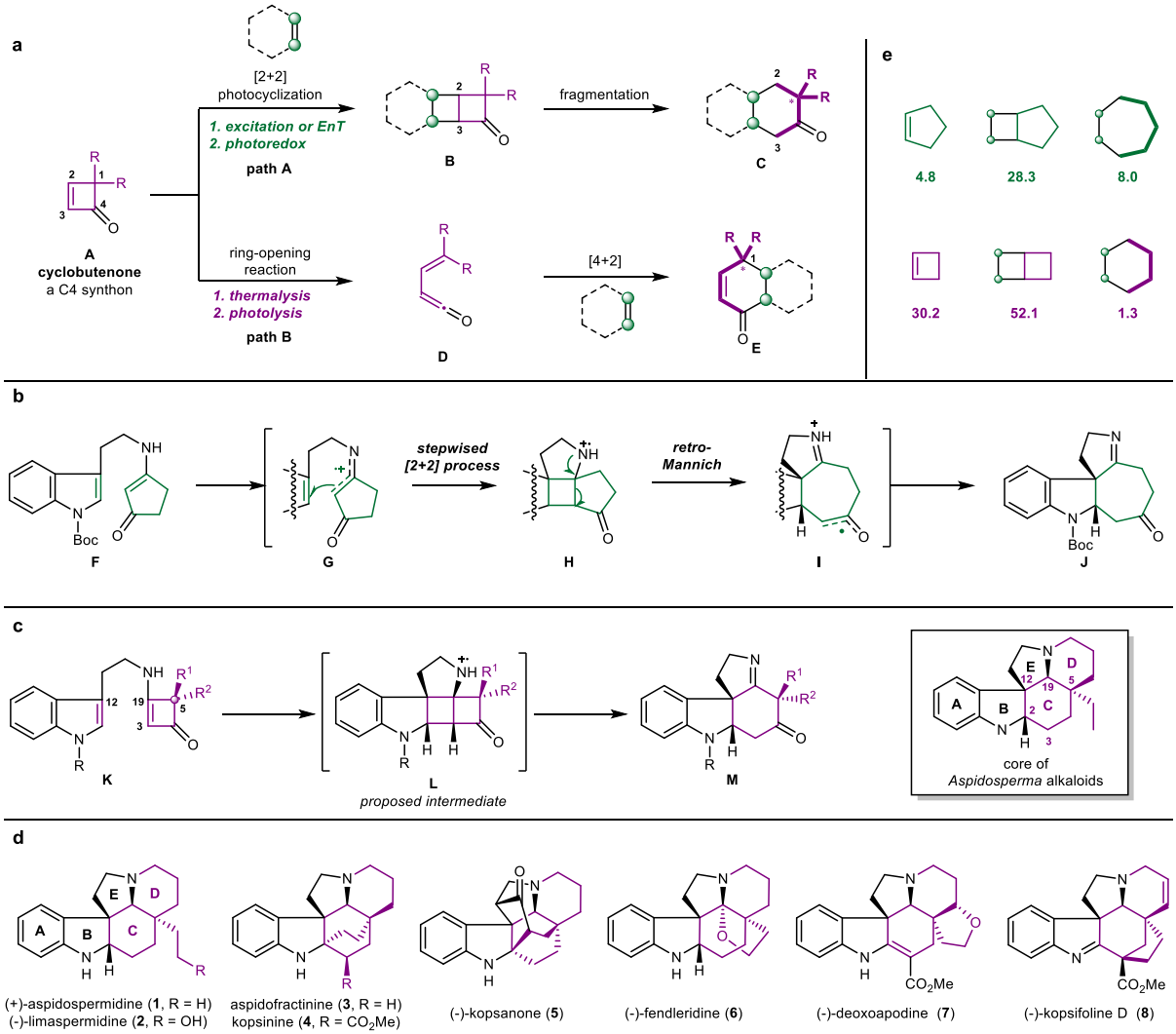

Figure 1. Synthetic Plan. a, general model of cyclobutanone bond cleavage. **b**, our previously reported method. **c**, plan for indole *Aspidosperma* alkaloid synthesis. **d**, naturally occurring *Aspidosperma* alkaloids. **e,** ring strain energy of cyclopentene, bicyclo[3.2.0]heptane, cycloheptane, cyclobutene, bicyclo[2.2.0]hexane and cyclohexane.

Herein, we report our recent contribution to the development of a novel strategy for stereoselective construction of the tetracyclic core of *Aspidosperma* alkaloids. Our method involves use of an Ir-catalysed PET reaction of **K** for stereoselective formation of the *cis*-configured BC bicyclic core with an all-carbon quaternary centre[25,26]. Computational studies suggest that the observed tandem PET reaction of **K** proceeds via an unusual 1,3-C shift to afford **M**, i.e. an interrupted [2+2] cyclization/retro-Mannich reaction.

Results and Discussion

Condition optimization

Our study commenced with evaluation of the proposed PET-based tandem [2+2] cyclization/retro-Mannich reaction. We selected compound **10a**, which has a spiro-pentacyclic core, as the target to be synthesized via the proposed PET reaction of substrate **9a** (Table 1), which can be synthesized from tryptamine and a substituted cyclobutane-1,3-dione according to a published protocol[27].

Initially, we focused on identifying catalysts that could promote the proposed PET reaction of **9a** on the basis of our previous results[15]. The reaction was performed in MeCN in the presence of photocatalysts under blue light-emitting diode (LED) irradiation at 30 °C. The results are listed in Table 1. Catalysts **I**[28], **II**[29], and **III**[30] gave the desired product **10a**; catalyst **I** gave the best result (Table 1, entries 1–3). The necessities of irradiation and photocatalyst were also defined (entries 4–5). However, use of the other tested catalysts did not give the desired products under the reaction conditions (see the Supplementary Information for details). Next, we evaluated the effects of different solvents on the production of **10a** in the presence of catalyst **I**. Changing the solvent to MeOH, tetrahydrofuran (THF), and dichloromethane (DCM) resulted in decreased yields and substrate conversions, and intense substrate

decomposition (entries 6–8). These results show that MeCN is the best solvent for the reaction.

Table 1. Condition screening[a].

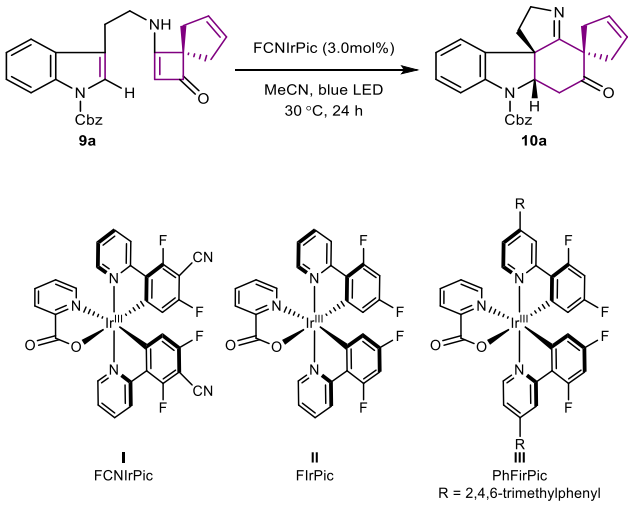

Entry	*Photocatalyst*	*Solvent*	*Temp.*	*Conv./Yield (%)*
1	FCNIrPic (**I**)	MeCN	30 ℃	100/90[a]
2	FirPic (**II**)	MeCN	30 ℃	83/26
3	PhFIrPic (**III**)	MeCN	30 ℃	65/43
4	In dark	MeCN	30 ℃	< 5/N. D.
5	No catalyst	MeCN	30 ℃	< 5/N. D.
6	FCNIrPic (**I**)	MeOH	30 ℃	84/23
7	FCNIrPic (**I**)	THF	30 ℃	30/20
8	FCNIrPic (**I**)	DCM	30 ℃	59/35
9	FCNIrPic (**I**)	MeCN	30 ℃	86/42[b]
10	FCNIrPic (**I**)	MeCN/PhMe	30 ℃	67/56[b,c]
11	FCNIrPic (**I**)	MeCN	10 ℃	100/60
12	FCNIrPic (**I**)	MeCN	20 ℃	100/66
13	FCNIrPic (**I**)	MeCN	40 ℃	90/50

Reaction conditions: A 15 mL glass vial was charged with 9a (0.1 mmol) and a photocatalyst (3.0 mol%) in an appropriate solvent (5.0 mL), and irradiated by two blue LEDs (centre wavelength, 455 nm; light intensity, 0.21 W/cm2). The yield and conversion were determined by ^{1}H NMR spectroscopy with 1,3,5-trimethoxybenzene as the internal standard. [a] Isolated yield = 86%. [b] -Cbz is replaced by -Boc (**9f**). [c] V_{MeCN}/V_{PhMe} = 10:1.

Finally, we investigated the effects of an N-substituent in the indole moiety, and of the reaction time and temperature, on the photocyclization results. Substrate **9f** was subjected to the optimized conditions, which resulted in both a lower conversion and yield (entry 9). In contrast, when the reaction of **9f** was performed in a mixed

MeCN/toluene (10:1) solvent, the conversion of substrate **9f** to product **10f** decreased, but the yield increased (56%) compared with that in entry 10 (42%). These results indicate that Cbz is a more effective protecting group than Boc under the profiled conditions. The effects of the reaction temperature on the outcomes of the PET reaction of **9a** were investigated. Among the conditions profiled (entries 11–13), the reaction in MeCN at 30 °C for 24 h gave the best result, namely quantitative conversion and 90% yield

Substrate scope

With the optimal conditions in hand, we then explored the substrate scope. Targeting on the total synthesis of *Aspidosperma* alkaloids, different tryptamine-substituted cyclobutenones (**9a**–**9n**) were prepared and reacted under the optimal conditions. The results are shown in Table 2; substrate **9a**, which contains a spiro-cyclopentene moiety, delivered the best result and gave **10a** in 86% isolated yield. When C15 or C16 was substituted with a chlorine atom, **10b** and **10c** were obtained in 70% and 72% yield, respectively. However, when C15 was substituted with a methyl group, the yield of **10d** decreased slightly to 63%. Product **10e**, which has two contiguous quaternary stereogenic centres (C2 and C3), was obtained in 74% yield without a significant change in the yield, which indicates that steric hindrance at C2 has a limited effect on the reactivity. However, when the steric hindrance of the protecting group was increased by replacing –Cbz by –Boc, the activity of the PET reaction decreased, which resulted in a lower yield of **10f** (55%). In the case of substrate **9g**, which has a stereogenic centre at C10, photocyclization afforded **10g** in moderate yield and with excellent diastereoselectivity (76% yield, d.r. > 20:1). This indicates that the reaction is controlled by the substrate conformation.

To investigate the effects of the spirocyclic ring size on the photocyclization, substrates **9h** and **9i** were prepared and subjected to the optimal conditions. The PET reaction of **9h** with a spiro-cyclohexene unit gave a pair of separable isomers, **10h-1** and **10h-2**, in 86% yield and a 1:1 ratio. The reaction of **9i**, which bears a spiro-cycloheptene moiety, afforded the annulated product **10i** in 67% yield. This indicates that an increase in the spirocyclic ring size negatively affects the photocyclization outcome. We expanded the reaction scope by synthesizing substrates **9j**–**9l**, which contain various types of saturated spirocycles. As anticipated, **10j**, **10k**, and **10l** were obtained in moderate yields (57%–66%) under the standard reaction conditions. When substrates **9m** and **9n**, which have a *gem*-dimethyl and *gem*-diethyl group, respectively, were used, their PET reactions required a longer reaction time to achieve full conversion. The resulting products **10m** and **10n** were obtained in yields of 62% and 58%, respectively.

Table 2. Substrate scope.

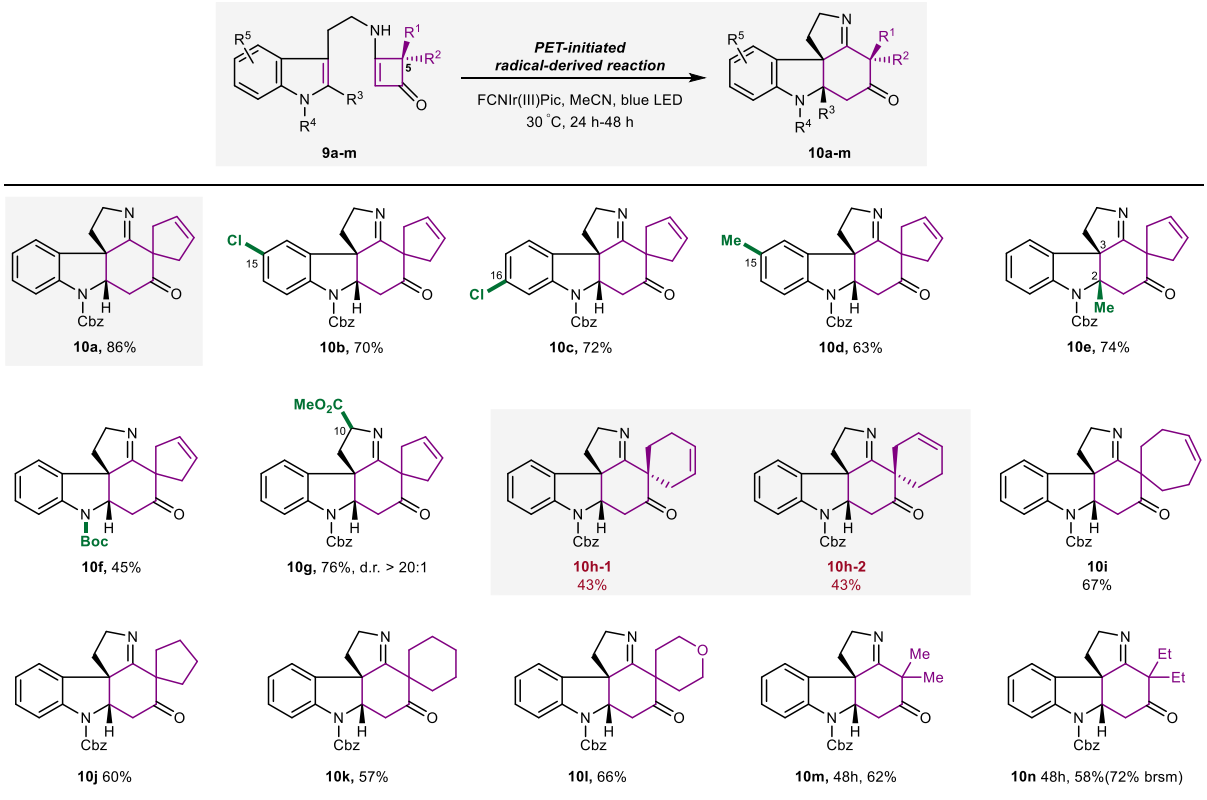

Computational study

The synthesis of (±)-aspidospermidine (**1**) and (±)-limaspermidine (**2**) showcased the effectiveness of our strategy for constructing complex monoterpene indole alkaloids[26]. In this work, we turned our attention to investigating the mechanistic intricacies of the key PET reaction for formation of the unique bicyclo[2.2.0]hexane unit present in the proposed intermediate **L** (Figure 1). In the presence of the excited photocatalyst [FCNIr(III)Pic]*, the substrate participates in an oxidative single-electron transfer (SET) process, which leads to the formation of **IN1**. The radical cation **IN1** served as the reference point for DFT investigations. As illustrated in Figure 2a, facilitated by a favourable radical cation–π interaction[31], **IN1** proceeds to the first radical addition transition state (**TS1**), with an energy barrier of 8.3 kcal/mol. This leads to the formation of benzyl radical **IN2**, which has a boat-like seven-membered ring. This structural feature may facilitate formation of the C19–C12 bond, even in the presence of critical steric hindrance between the C5 quaternary carbon and the indole moiety.

Further DFT investigation proved challenging because of the peculiar features that the potential energy surface (PES) exhibits in the rate-determining step, which involves both formation of the C19–C12 bond and cleavage of the C19–C3 bond. This process has an energy barrier of 21.8 kcal/mol via **TS2**, and results in direct formation of **IN3**, which can undergo reductive SET in the presence of $[FCNIr(II)Pic]^{-}$. This leads to the regeneration of [FCNIr(III)Pic] to complete the catalytic cycle and formation of the final product via proton transfer. Intrinsic reaction coordinate (IRC) analysis showed the reaction coordinate connecting the transition state **TS2**, the reactant (**IN2**), and the C19–C3 bond cleavage product **IN3** wells (Figure 2c).

Possible intermediates with a bicyclo[2.2.0]hexane unit located on the PES minimum were investigated by performing two-dimensional scans of simplified structures to find a minimum. When the nonbonding sp^3 orbital of the N atom is positioned antiperiplanar to the adjacent C19–C3 bond, an intermediate **IN4** with a bicyclo[2.2.0]hexane unit was successfully located. However, the Gibbs free energy of **IN4 (**$\Delta G°$ = +27.4 kcal/mol) is significantly higher than the activation energy of **TS2** ($\Delta G^{\neq}$ = 22.4 kcal/mol). This energy difference can be attributed to a subtle discrepancy between the spin localizations of **IN4** and **TS2**. As depicted in Figure 2b, the spin density of **IN4** is predominantly concentrated at the benzene ring, whereas in **TS2** it is primarily localized at C19, C12, C3, and N9 (Figure 2a)[32]. Therefore, the intermediacy of IN4 was ruled out.

We assume that the overlap between the sp^2-hybridized N spin centre and σ*(C19–C3) in **TS2**, and the ring-strain release of the transient bicyclo[2.2.0]hexane unit, play essential roles that enable the reaction to occur. Thus, natural bond orbital (NBO)[33] and Mayer bond order[34,35] analyses were performed to determine the hyperconjugative interactions in the intermediates, transition states, and transient structures along the IRC path (Figure 2c and 2d). In the early stage of this process (Figure 2f, **IN2** → **R-50** → **R-24** → **TS2**), formation of the C19–C3 bond arises from the orbital overlap between the p orbital of the C19 atom (Figure 2e, **R-24**) and the $\pi_{(C3=N9)}$* orbital. During this process, the bond order of C19–C12 increases, but no significant change is observed for C19–C3. This leads to formation of a nonbonding p orbital at the N9 atom (Figure 2e, **F-10**). Further geometrical adjustment and conformational restriction of the transient structure enable the N9 nonbonding p orbital to align parallel to the $\sigma_{(C19–C3)}$* orbital (Figure 2f, **TS2** → **F-10** → **F-40** → **IN3**), which reinforces the hyperconjugative interaction. Facilitated by the bond stretching and bond-angle bending of the transient structure with a pseudo bicyclo[2.2.0]hexane unit,

the favourable hyperconjugative interaction ultimately leads to cleavage of the C19–C3 bond (**TS2** → **IN3**) and release of the ring strain.

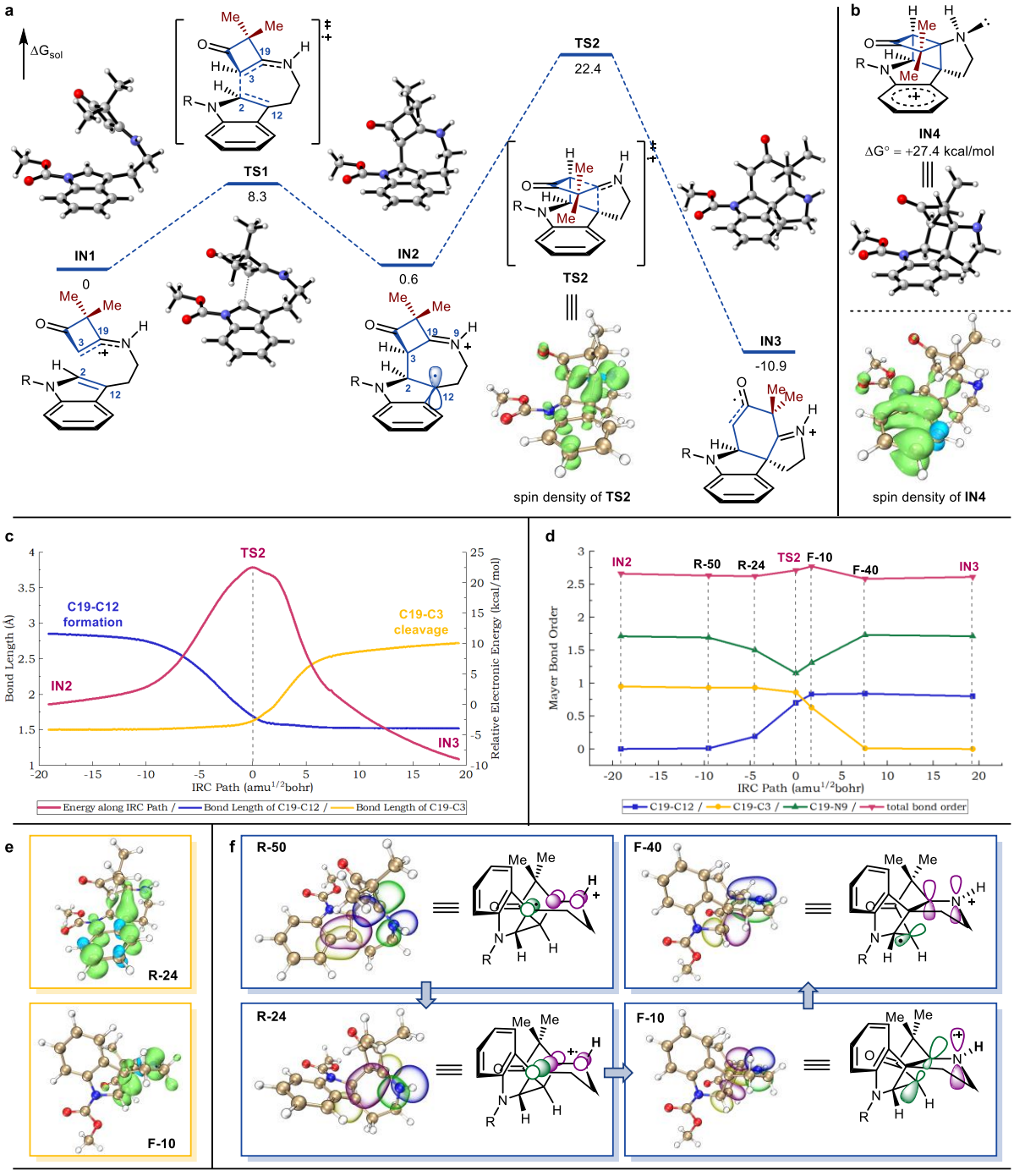

Fig. 2. Computational study. a, energy profiles from **IN1** to **IN3** and spin density of **TS2** (isovalue = 0.004), solvated (SMD) Gibbs free energies were calculated at the B3LYP-D3/def2-tzvp//B3LYP/6-31G(d) level in MeCN. **b**, spin density of **IN4** (isovalue = 0.004). **c**, IRC analysis of **TS2** (red line) and bonds length changes of C19-C3 (yellow line) and C19-C12 (blue line) along IRC path. **d**, Mayer bond order changes of selected structures along IRC path. **e,** spin density analyses of **R-24** and **F-10** (isovalue = 0.004). **f,** NBO analyses of the selected transient structures (isovalue = 0.04).

DFT analysis hereby declare that the orbital symmetry involved in this process does not conform to a sigmatropic rearrangement reaction[36]. Inspection of the changes in the bond lengths (Figure 2c) and Mayer bond orders (Figure 2d) along the IRC path clearly show that C19–C12 bond formation and C19–C3 bond cleavage are asynchronous. On the basis of these premises, we assume that the process **IN2** → **IN3** is neither strictly concerted nor stepwise. This can be attributed to the inherent ring-strain release in the transient structure located on the PES and the hyperconjugative interaction between the N9 nonbonding p orbital and $\sigma_{(C19\text{-}C3)}$* during geometrical distortions. This ambiguous mechanistic feature suggests an unusual 1,3-C shift, and indicates that this reaction proceeds via a PET-initiated interrupted [2+2]/retro-Mannich process.

Conclusion

In summary, a PET-initiated cationic radical-derived interrupted [2+2]/retro-Mannich reaction has been developed for constructing the ABCE tetracyclic cores of Aspidosperma alkaloids from tryptamine-substituted cyclobutenones. The functionalized C5 atom in the formed ABCE tetracyclic core provides potential opportunities for accessing more complex indole alkaloids. The extensive DFT study indicated that the observed PET-initiated cationic radical-derived reaction proceeds via an unconventional formal 1,3-C shift, which is neither concerted nor stepwise. These findings shed light on the mechanistic innovation of a PET-initiated radical-derived reaction that was driven by the ring strain releasing.

Supporting Information

Supporting Information File 1:

Experimental procedures, characterization data, NMR spectra, and computational study.

Acknowledgements

This work was supported by the National Science Foundation of China (Grant Nos. 22171013), Guangdong Natural Science Foundation (Grant Nos. 2020B0303070002), Shenzhen Basic Research Program (Grant No. JCYJ 20180302180215524), Shenzhen-Hong Kong Institute of Brain Science-Shenzhen Fundamental Research Institutions (2024SHIBS0004), Key Laboratory of Structure-Based Drug Design & Discovery of Ministry of Education,Shenyang Pharmaceutical Universit (SY2024KF-02), the research grants from the Major Program of Shenzhen Bay Laboratory, and the Shenzhen Outstanding Talents Training Fund.

ORCID® iDs

Zhong-Chao Zhang - 0000-0001-5017-5691

Zhen Yang - 0000-0001-8036-934X

Data Availability Statement

All data that supports the findings of this study is available in the published article and/or the supporting information of this article.

References

1. Bach, T.; Hehn, J. P. Photochemical reactions as key steps in natural product synthesis. *Angew. Chem., Int. Ed.* **2011**, *50*, 1000−1045.

2. Kärkäs, M. D.; Porco, J. A.; Stephenson, C. R. Photochemical approaches to complex chemotypes: Applications in natural product synthesis. *Chem. Rev.* **2016**, *116*, 9683−9747.

3. Pitre, S. P. ;Overman, L. E. Strategic use of visible-light photoredox catalysis in natural product synthesis. *Chem. Rev.* **2022**, *122*, 1717−1751.

4. Winkler, J. D.; Bowen, C. M.; Liotta, F. [2+2] Photocycloaddition/fragmentation strategies for the synthesis of natural and unnatural products. *Chem. Rev.* **1995**, *95*, 2003–2020.

5. Baldwin, J. E. *Comprehensive Organic Synthesis* (Pergamon Press, 1991).

6. Poplata, S.; Tröster, A.; Zou, Y.-Q.; Bach, T. Recent advances in the synthesis of cyclobutanes by olefin [2 + 2] photocycloaddition reactions. *Chem. Rev.* **2016**, *116*, 9748−9815.

7. Großkopf, J.; Kratz, T.; Rigotti, T.; Bach, T. Enantioselective photochemical reactions enabled by triplet energy transfer. *Chem. Rev.* **2021**, *122*, 1626–1653.

8. For original papers of PET reaction, see: Takahashi, Y.; Okitsu, O.; Ando, M.; Miyashi, T. Electron transfer induced intramolecular [2+2] cycloaddition of 2,6-diarylhepta-1,6-dienes. *Tetrahedron Lett.* **1994**, *35*, 3953−3956.

9. Ravelli, D.; Protti, S.; Fagnoni, M. Carbon-carbon bond forming reactions via photogenerated intermediates. *Chem Rev.* **2016**, *116*, 9850–9913.

10. Romero, N. A.; Nicewicz, D. A. Organic photoredox catalysis. *Chem. Rev.* **2016**, *116*, 10075−10166.

11. Chen, P. H.; Dong, G. Cyclobutenones and benzocyclobutenones: versatile synthons in organic synthesis. *Chem. Eur. J.* **2016**, *22*, 18290-18315.

12. Wiberg, K. B. The concept of strain in organic chemistry. *Angew. Chem., Int. Ed.* **1986**, *25*, 312−322.

13. Paquette, L. A.; Schwartz, J. A. Stereochemical course of the thermally induced fragmentation of bicyclo[2.2.0]hexanes to diallyls. pyrolysis of the dimethyl bicyclo[2.2.0]hexane-2,3-dicarboxylates. *J. Am. Chem. Soc.* **1970**, *92*, 3215.

14. Wilson, S. R.; Phillips, L. R.; Pelister, Y.; Huffman, J. C. Cyclobutene derivatives as isoprene equivalents in terpene synthesis. 3. bicyclo[2.2.0]hexanes. *J. Am. Chem. Soc.* **1979**, *101*, 7373–7379.

15. Mu, X.-P.; Li, Y.-H.; Zheng, N.; Long, J.-Y.; Chen, S.-J.; Liu, B.-Y.; Zhao, C.-B.; Yang, Z. Stereoselective synthesis of cyclohepta[b]indoles by visible-light-induced [2+2]-cycloaddition/ retro-Mannich-type reactions. *Angew. Chem., Int. Ed*. **2021**, *60*, 11211–11216.

16. Schell, F. M.; Cook, P. M. Intramolecular photochemistry of a vinylogous amide and some transformations of the photoproduct. *J. Org. Chem.* **1984**, *49*, 4067–4070.

17. Winkler, J. D.; Muller, C. L.; Scott, R. D. A new method for the formation of nitrogen-containing ring systems via the intramolecular photocycloaddition of vinylogous amides. A synthesis of mesembrine. *J. Am. Chem. Soc*. **1988**, *110*, 4831–4832.

18. Zhu, M.; Zhang, X.; Zheng, C.; You, S. L. Energy-transfer-enabled dearomative cycloaddition reactions of indoles/pyrroles via excited-state aromatics. *Acc. Chem. Res*. **2022**, *55*, 2510–2525 and references cited therein.

19. Zhao, S.; Sirasani, G.; Andrade, R. B. *The Alkaloids: Chemistry and Biology* (Elsevier, 2021).

20. Sears, J. E.; Boger, D. L. Tandem intramolecular Diels–Alder/1, 3-dipolar cycloaddition cascade of 1, 3, 4-oxadiazoles: initial scope and applications. *Acc. Chem. Res*. **2016**, *49*, 241-251.

21. Pritchett, B. P.; Stoltz, B. M. Enantioselective palladium-catalyzed allylic alkylation reactions in the synthesis of Aspidosperma and structurally related monoterpene indole alkaloids. *Nat. Prod. Rep*. **2018**, *35*, 559–574.

22. Wang, Y.; Xie, F.; Lin, B.; Cheng, M.; Liu, Y. Synthetic approaches to tetracyclic indolines as versatile building blocks of diverse indole alkaloids. *Chem. Eur. J.* **2018**, *24*, 14302–14315.

23. Saya, J. M.; Ruijter, E.; Orru, R. V. A. Total synthesis of Aspidosperma and Strychnos alkaloids through indole dearomatization. *Chem. Eur. J.* **2019**, *25*, 8916–8935.

24. Ring strain energy calculations were performed in B3LYP-D3/def2-SVP level according to the reported method: Khoury, P. R.; Goddard, J. D.; Tam, W. Ring strain energies: substituted rings, norbornanes, norbornenes and norbornadienes. *Tetrahedron* **2004**, *60*, 8103−8112.

25. Quasdorf, K. W.; Overman, L. E. Catalytic enantioselective synthesis of quaternary carbon stereocentres. *Nature* **2014**, *516*, 181−191.

26. The developed chemistry has been successfully applied to the total syntheses of aspidospermidine **(1)** and limaspermidine **(2)** by our group, see: Long, J.-Y.; Liu, R.-D.; Mu, X.-P; Song, Z.-L.; Zhang, Z.-C.; Yang, Z. Development of a Strategy for the Total Synthesis of Aspidosperma Alkaloids via the Cyclobutenone-Based PET-Initiated Cationic Radical-Driven [2+2]/Retro-Mannich Reaction. *Org. Lett*. **2024**, *26*, 2960−2964.

27. Brand, S.; de Candole, B. C.; Brown, J. A. Efficient synthesis of 3-aminocyclobut-2-en-1-ones: squaramide surrogates as potent VLA-4 antagonists. *Org. Lett.* **2023**, *5*, 2343–2346.

28. D'Andrade, B. W.; Datta, S.; Forrest, S. R.; Djurovich, P.; Polikarpov, E.; Thompson, M. E. Relationship between the ionization and oxidation potentials of molecular organic semiconductors. *Org. Elect.* **2005**, *6*, 11-20.

29. Adachi, C.; Kwong, R. C.; Djurovich, P.; Adamovich, V.; Baldo, M. A.; Thompson, M. E.; Forrest, S. R. Endothermic energy transfer: A mechanism for generating very efficient high-energy phosphorescent emission in organic materials. *App. Phys. Lett.* **2021**, *79*, 2082-2084.

30. Kozhevnikov, V. N.; Zheng, Y.; Clough, M.; Al-Attar, H. A.; Griffiths, G. C.; Abdullah, K.; Raisys, S.; Jankus, V.; Bryce, R. B.; Monkman, A. P. Cyclometalated Ir (III) complexes for high-efficiency solution-processable blue PhOLEDs. *Chem. Mater.* **2013**, *25*, 2352-2358.

31. Yamada, S. Cation−π interactions in organic synthesis. *Chem. Rev.* **2018**, *118*, 11353−11432.

32. Spin density and NBO orbitals were rendered by VMD: Humphrey, W.; Dalke, A.; Schulten, K. VMD: Visual molecular dynamics. *J. Mol. Graphics* **1996**, *14*, 33−38.

33. NBO 7.0. Glendening, E. D.; Badenhoop, J. K.; Reed, A. E.; Carpenter, J. E.; Bohmann, J. A.; Morales, C. M.; Karafiloglou, P.; Landis, C. R. and Weinhold, F. Theoretical Chemistry Institute, University of Wisconsin, Madison, WI (2018).

34. Mayer, I. Charge, bond order and valence in the AB initio SCF theory. *Chem. Phys. Lett.* **1983**, *97*, 270−274.

35. Lu, T.; Chen, F. Multiwfn: A multifunctional wavefunction analyzer. *J. Comput. Chem.* **2012**, *33*, 580−592.

36. Woodward, R. B. & Hoffmann, R. *The conservation of orbital symmetry.* (Weinheim: Verlag Chemie, 1970).